In Situ Formed Lithium Sulfide/Microporous Carbon Cathodes for Lithium-Ion Batteries

Shiyou Zheng,[†,‡] Yvonne Chen,[§] Yunhua Xu,[‡] Feng Yi,[⊥] Yujie Zhu,[‡] Yihang Liu,[‡] Junhe Yang,[†,*] and Chunsheng Wang[‡,*]

[†]School of Materials Science and Engineering, University of Shanghai for Science & Technology, Shanghai 200093, China, [‡]Department of Chemical and Biomolecular Engineering, University of Maryland, College Park, Maryland 20742, United States, [§]Space and Defense Division, Saft America Inc., Cockeysville, Maryland 21030, United States, and [⊥]Material Measurement Laboratory, National Institute of Standards and Technology, Gaithersburg, Maryland 20899, United States

ABSTRACT Highly stable sulfur/microporous carbon (S/MC) composites are prepared by vacuum infusion of sulfur vapor into microporous carbon at 600 °C, and lithium sulfide/microporous carbon (Li_2S/MC) cathodes are fabricated *via* a novel and facile *in situ* lithiation strategy, *i.e.*, spraying commercial stabilized lithium metal powder (SLMP) onto a prepared S/MC film cathode prior to the routine compressing process in cell assembly. The *in situ* formed Li_2S/MC film cathode shows high Coulombic efficiency and long cycling stability in a conventional commercial Li-ion battery electrolyte (1.0 M $LiPF_6$ + EC/DEC (1:1 v/v)). The reversible capacities of Li_2S/MC cathodes remain about 650 mAh/g even after 900 charge/discharge cycles, and the Coulombic efficiency is close to 100% at a current density of 0.1C, which demonstrates the best electrochemical performance of Li_2S/MC cathodes reported to date. Furthermore, this Li_2S/MC film cathode fabricated *via* our *in situ* lithiation strategy can be coupled with a Li-free anode, such as graphite, carbon/tin alloys, or Si nanowires to form a rechargeable Li-ion cell. As the Li_2S/MC cathode is paired with a commercial graphite anode, the full cell of Li_2S/MC-graphite (Li_2S-G) shows a stable capacity of around 600 mAh/g in 150 cycles. The Li_2S/MC cathodes prepared by high-temperate sulfur infusion and SLMP prelithiation before cell assembly are ready to fit into current Li-ion batteries manufacturing processes and will pave the way to commercialize low-cost Li_2S-G Li-ion batteries.

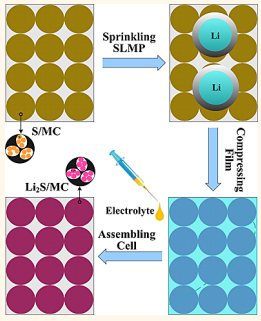

KEYWORDS: Li-ion battery · lithium−sulfur · Li_2S · microporous carbon

Lithium−sulfur (Li−S) batteries are considered to be a promising candidate for next-generation lithium batteries owing to their high theoretical specific capacity (1675 mAh/g) and high energy density (2600 Wh/kg).[1−3] Li−S batteries utilize elemental sulfur as the active cathode material to reversibly react with metal lithium as

$$S_8 + 16Li^+ + 16e^- \leftrightarrow 8Li_2S \qquad (1)$$

Sulfur is naturally abundant, low-cost, and environmentally friendly. However, the commercialization of Li−S batteries faces the following challenges: (i) low active material utilization due to the insulating nature of sulfur and solubility of lithium polysulfide intermediates (Li_2S_x, $4 \le x \le 8$) in liquid electrolytes,[4,5] (ii) poor cycle life and low Coulombic efficiency arising from the dissolved lithium polysulfide shuttle and large volume change of the sulfur cathode during lithiation/delithiation,[6,7] and (iii) the use of a metal lithium anode creates known safety issues with liquid electrolytes.[8,9]

A variety of strategies have been pursued to circumvent the sulfur cathode problems. The most effective methods are optimization of organic electrolytes[10−14] and fabrication of sulfur-conductive polymer composites[15−17] and sulfur−carbon-based composites.[18−22] Among them, sulfur−porous carbon nanocomposites are more attractive because porous carbon can (1) improve the electronic conductivity, (2) accommodate volume change, and (3) suppress the dissolution of polysulfides.[23−25] Nazar *et al.*[26] reported that a nanostructured sulfur−-mesoporous carbon cathode showed stable and reversible capacity. Manipulation of the pore size[27−29] and structure of carbon materials (nanotubes,[30−32] graphene,[33−35] and carbon hybrids[36]) can further improve the electrochemical performance of Li−S batteries. We developed a highly stable S/C cathode by infusing short-chain S_2 into

* Address correspondence to cswang@umd.edu; jhyang@usst.edu.cn.

Received for review September 3, 2013 and accepted November 19, 2013.

Published online November 19, 2013
10.1021/nn404601h

microporous carbon at a high temperature, which effectively prevented the formation of high-order polysulfides during lithiation, thus significantly improving the Coulombic efficiency and cycling stability of the S cathode.[32] In addition, the absence of high-order polysulfides will allow using low-cost carbonate-based electrolytes since the side reaction between the carbonate solvent and polysulfide anions is avoided.[12]

Although great advances have been made in stabilizing the S cathode, the cycling stability and Columbic efficiency of these S cathodes are still lower than current ceramic ones. Moreover, all of these superior S-based composite cathodes do not contain Li and still require metal lithium or lithiated anodes for the redox couple. Today, metal lithium anodes are not used in liquid electrolyte secondary batteries due to the inevitable formation of lithium dendrites during cycling. The formation of lithium dendrites will lead to poor cyclic performance and increase the probability of internal short circuit, thus resulting in safety issues.[8,9] To mitigate the safety problem of Li–S batteries, a few researchers have explored the possibility of preparing Li_2S–C composites as cathodes.[37−40] Currently, Li_2S–C composites are synthesized using complex wetting chemistry,[37] high-energy dry ball milling,[38,40] and carbonization of polyaniline–Li_2S_x.[39] Since Li_2S is thermodynamically unstable in air due to moisture, Li_2S–C materials have to be synthesized in a protected atmosphere. Due to the high humidity sensitivity of Li_2S materials, the Li_2S–C composite cathodes fabricated using the above methods showed poor cycling stability during prolonged cycling, which limited the practical applications of Li_2S–C cathodes for Li-ion batteries.

In the present work, a superior stable sulfur/microporous carbon (MC) cathode in a low-cost carbonate-based electrolyte was synthesized by infusing small sulfur molecule (S_2) vapor into MC under vacuum at 600 °C. The fabricated S/MC composite cathode was then prelithiated by spraying stabilized lithium metal powder (SLMP) onto the S/MC cathode film followed by compressing (*i.e.*, a routine step in the cell manufacturing process) prior to cell assembly, which is a novel and facile *in situ* technique. The SLMP has a Li content of 98% and is air stable and safe to be handled in ambient conditions. Once the outer protective shell of the SLMP is broken by applying mechanical force on the SLMP/S/MC electrode, the Li can be released and the activated Li can quickly transport through a 3D carbon matrix and uniformly react with S in porous carbon to form Li_2S *in situ* (Scheme 1), as evidenced by the uniform distribution of potentials with 1.0 V (*vs* Li/Li^+) in different locations of the as-prepared Li_2S/MC film electrodes when they are tested in half-cells. The extra SLMP can be added to a Li_2S/MC cathode to compensate for the first irreversible capacity of anode, which is very important for coupling with high-capacity Si and Sn anodes. Surprisingly, the Li_2S/MC cathode shows stable, high capacities together with good rate and long cycling stability in a conventional commercial Li-ion battery electrolyte (1.0 M $LiPF_6$ in a mixture of ethylene carbonate/diethyl carbonate (EC/DEC, 1:1 by volume)). Furthermore, this Li_2S/MC film cathode prepared *via* an *in situ* strategy can be coupled with a Li-free anode, such as graphite, carbon/tin alloys, or Si nanowires to form a "true" rechargeable Li-ion cell. A commercial graphite was chosen as a model anode to pair with the Li_2S/MC cathode, forming a Li_2S–graphite (Li_2S–G) full cell, which shows high capacity and long cycling stability. The technology reported will play a significant role in the commercialization of Li_2S cathodes for low-cost and high-energy Li-ion batteries.

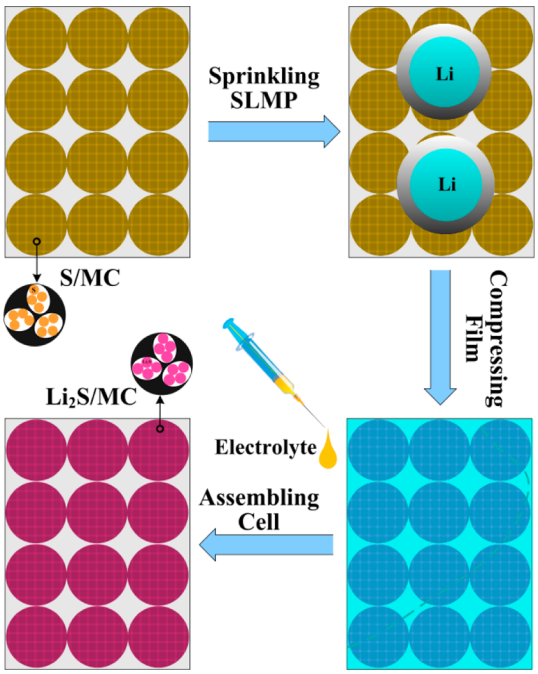

Scheme 1. Schematic illustration of *in situ* fabrication process of a Li_2S/MC composite electrode.

RESULTS AND DISCUSSION

Structure Analysis. The phase structure of the S/MC composite powders was characterized by X-ray diffraction (XRD). To index the sulfur and microporous carbon in the S/MC composite, the XRD of a physical mixture of S and MC (denoted as mixed S–MC hereafter) with the same composition as the S/MC, pure S, and MC was also tested as control. XRD patterns of the samples for S, MC, mixed S–MC, and S/MC are compared in Figure 1a. As expected, the peaks belonging to S_8 crystalline phases are not observed in the S/MC composite (curve b), whose pattern is almost identical to that of the MC (curve a), showing only two broad peaks within the range of 20–50° from the amorphous carbon. This result suggests that XRD cannot detect the short-chain phase (S_2) in the S/MC composite,[32] while

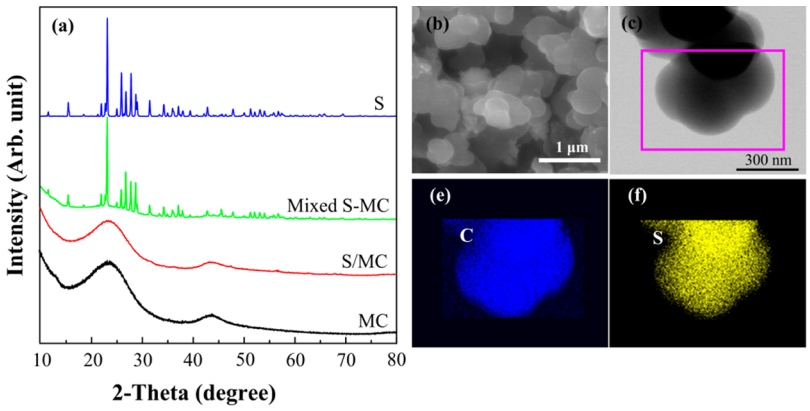

Figure 1. (a) XRD patterns of MC, S/MC, mixed S−MC, and S, (b) SEM image of S/MC composite powder, (c) TEM image of S/MC composite, and the corresponding EDS mapping of C (e) and S (f) for the marked region in image (c).

in the case of mixed S−MC, the sharp and intense peaks from the S_8 crystal are clearly visible. It was reported that at 600 °C 99% of S_8 will break into S_2, and these S_2 would strongly interact with the surface and fill the first micropores and then form a mono- or few-layered coverage of the matrix particle surface.[41] When the temperature is cooled to room temperature, the S phases inside the micropores remain as the state of S_2.[42−44] The XRD fails to detect S_2 peaks in MC either because S_2 in the pores of carbon is an ultrathin layer or because S is amorphous. The scanning electron microscopy (SEM) and transmission electron microscopy (TEM) images of the resulting S/MC composite and the corresponding energy-dispersive X-ray spectrometry (EDS) C and S maps are displayed in Figure 1b−f. The S/MC composite powder has a spherical shape with a particle size of about 600 nm. The elemental mapping images of C and S in Figure 1e and f show that the S map covers the C map. This clearly indicates that the sulfur is well dispersed in the S/MC composite.

The morphologies of the S/MC, SLMP-sprinkled S/MC (SLMP/S/MC), and compressed SLMP/S/MC electrode films are presented in Figure 2a−c. For the pristine S/MC electrode film, the S/MC particles were uniformly coated on the Al current collector to form a porous structure, as show in Figure 2a. After sprinkling SLMP, the SLMP spheres spread onto the surface of the S/MC electrode film and remain intact with the S/MC electrode due to the inert coating layer on the Li metal (Figure 2b). The particle size of the SLMP spheres is around 50 μm. Undergoing mechanical compression, these SLMP spheres are pressed down evenly and imbedded into the S/MC composite electrode; see Figure 2c. That is, the active Li can be released by breaking the outer protective shell of the SLMP and react with the active material sulfur. The variation of phase components for the S/MC electrode film before and after the introduction of SLMP was also determined by XRD. The XRD patterns of the pristine S/MC film, SLMP/S/MC film, compressed SLMP/S/MC film, and the compressed SLMP/S/MC film with a drop of electrolyte are shown in Figure 2d. As compared to the pristine S/MC electrode film, a metal Li peak at around 36 degrees is clearly visible in the SLMP/S/MC film sample because of the load of SLMP (curve (ii) in Figure 2d). After mechanical compression, the peak belonging to the Li phase became weak and an new peak at 26.8 degrees (marked by a heart in curve (iii) of Figure 2d) appeared; the new peak can be indexed as (111) of Li_2S. The coexistence of Li and Li_2S phases implies that the Li is activated and Li_2S can be *in situ* formed by solid phase reaction but not completely. After a very small amount of electrolyte is dropped on the compressing SLMP/S/MC film, the Li peak becomes invisible and the intensity of the Li_2S peak increases, suggesting that the active Li reacts with the S in the S/MC composite and completely transforms to Li_2S in the electrolyte environment. The XRD results verify the feasibility of *in situ* fabrication of Li_2S in the sulfur-containing electrodes. Therefore, the Li in SLMP will completely react with S in MC to form a Li_2S/MC cathode after cell assembly.

Electrochemical Properties. The electrochemical performances of the Li_2S/MC electrode were characterized in a coin cell using Li metal foil as the counter and reference electrode and 1.0 M $LiPF_6$ in EC/DEC (1:1 v/v) as the electrolyte. The initial three-cycle lithiation/delithiation behaviors of the pristine S/MC and as-prepared Li_2S/MC electrodes were characterized using cyclic voltammetry (CV), shown in Figure 3. For the pristine S/MC electrode, the open-circuit potential of the cell is around 3.0 V (*vs* Li/Li^+); during the catholic scan (lithiation), the cell exhibits two cathodic peaks at about 2.4 and 1.1 V (*vs* Li/Li^+) in the first cycle, as shown in Figure 3a. The small peak at high voltage of 2.4 V (*vs* Li/Li^+) is associated with the formation of soluble high-order polysulfides through lithiation of the minor resident S_8 on the outside surface of porous carbon based on eqs 2−4:

$$S_8 + 2e^- \rightarrow S_8^{2-} \quad (2)$$

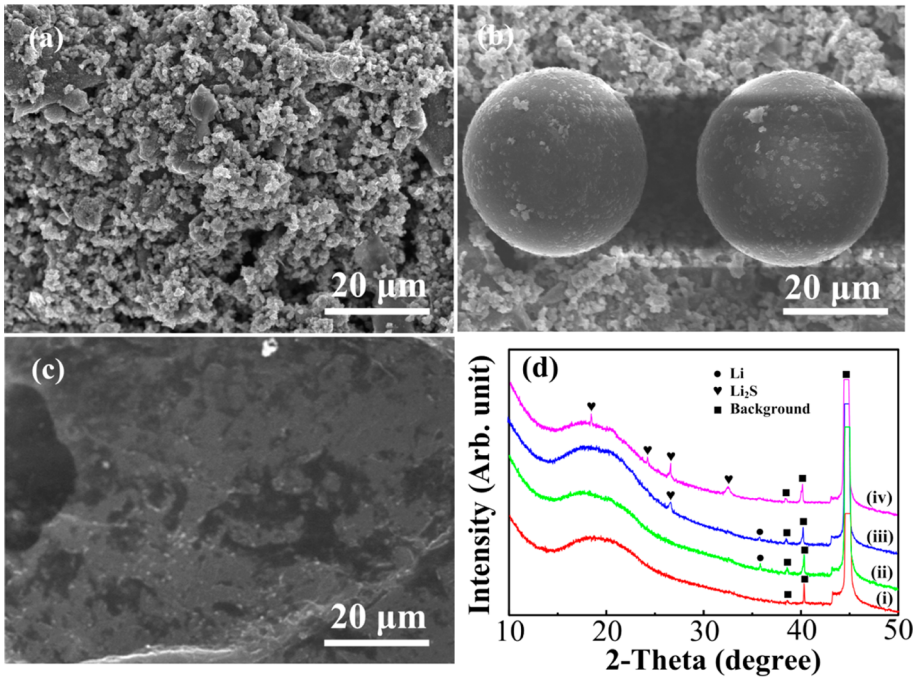

Figure 2. (a) SEM image of the pristine S/MC electrode film, (b) SEM image of the SLMP-sprinkled S/MC electrode film, (c) SEM image of the compressed SLMP/S/MC electrode film, and (d) XRD patterns of the S/MC electrode film before and after sprinkling SLMP: (i) pristine S/MC electrode, (ii) SLMP-sprinkled S/MC electrode, (iii) compressed SLMP/S/MC electrode, and (iv) compressed SLMP/S/MC electrode after electrolyte is dropped.

$$3S_8^{2-} + 2e^- \rightarrow 4S_6^{2-} \quad (3)$$

$$2S_6^{2-} + 2e^- \rightarrow 3S_4^{2-} \quad (4)$$

The small cathodic peak at 2.4 V (*vs* Li/Li^+) vanishes in the flowing cycles, which may be attributed to dissolution of a small amount of high-order polysulfides into the electrolyte and potential side reaction between polysulfide anions and carbonate solvent.[45]

The low-voltage peak at 1.1 V (starting at 1.8 V (*vs* Li/Li^+)) is related to formation of insoluble low-order polysulfides as

$$S_4^{2-} + 2Li^+ \rightarrow 2Li_2S_2 \quad (5)$$

$$Li_2S_2 + 2Li^+ + 2e^- \rightarrow 2Li_2S \quad (6)$$

The second peak is broad and appears at a low voltage, which is probably due to the physical or chemical interaction between S_2 and porous carbon.[32] The S_2 in porous carbon was formed by the breakage of S_8 at 600 °C, and then these S_2 were infused into the micropores of the porous carbon and were stabilized at room temperature due to the restriction of pore size and interaction between S_2 and carbon, but the S_2 absorbed on the outside of carbon changed back to S_8 when the temperature cooled to room temperature.[41,42,44] After the first cycle, the low-voltage peak current near 1.1 V (*vs* Li/Li^+) was significantly reduced and shifted toward a more positive direction due to volume change. A positive voltage shift was also observed for high-capacity Si and metal oxide electrodes with a large volume change.[46] The low voltage in the first lithiation scan is attributed to large strain/stress since a large volume change requires a large overpotential, while the strain/stress was reduced in the second lithiation due to the introduction of large defects in the electrode and pore size expansion of carbon in the first lithiation, thus reducing the overpotential and shifting the voltage to high voltage in the second lithiation.[47] For the anodic scan, only one peak, at 2.0 V (*vs* Li/Li^+), associated with oxidation of Li_2S back to S_4 or S_2, can be observed. However, for the as-prepared Li_2S/MC, the cell shows an open-circuit potential of 1.0 V (*vs* Li/Li^+) (Figure 3b), further confirming the formation of Li_2S in MC. Contrary to the S/MC electrodes, the Li_2S/MC cathode has to be delithiated first. As the Li_2S/MC cathode was scanned from an open-circuit of 1.0 toward 3.0 V (*vs* Li/Li^+), only one anodic peak, at 2.0 V (*vs* Li/Li^+), and one cathodic peak, at 1.6 V (*vs* Li/Li^+), were observed. The current and potential of both the cathodic and the anodic peaks are very stable except that the current of the cathodic peak in the initial cycle is slightly higher than that in the following delithiation scans. This suggests that the *in situ* formed Li_2S/MC do not have an activation process reported in the ball-milled Li_2S–C cathode[37] and observed in pristine S/MC (Figure 3a). The stable cathodic current peaks in the first and following cathodic scans also demonstrate that the large irreversible capacity in the S/MC cathode has been compensated by the SLMP in the Li_2S/MC cathode during the prelithiation process.

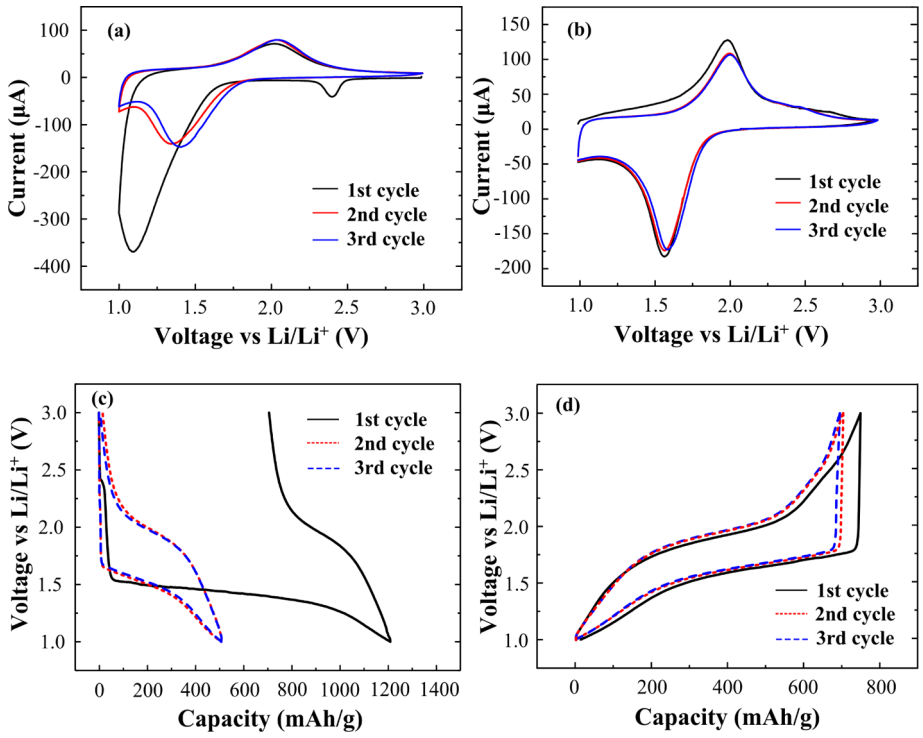

Figure 3. Cyclic voltammograms and discharge/charge voltage profiles of the electrodes in the first three cycles at 0.1C: (a and c) for the pristine S/MC and (b and d) for the as-prepared Li_2S/MC.

The first three charge/discharge cycles at 0.1C (1C = 1675 mA/g) of the S/MC and as-prepared Li_2S/MC electrodes are also compared in Figure 3. The discharge/charge curves of the S/MC electrode show a very short plateau at 2.4−2.5 V (*vs* Li/Li^+) and a long plateau at 1.7 V (*vs* Li/Li^+) in the first discharge and only one plateau at 2.0 V (*vs* Li/Li^+) in the charge (Figure 3c). The short plateau at 2.4−2.5 V (*vs* Li/Li^+) disappeared in the second discharge due to dissolution of a small amount of high-order polysulfides. The lithiation capacity is around 1200 mAh/g in the first cycle, 510 mAh/g in the second cycle, and approximately 508 mAh/g in the third cycle for the pristine S/MC cathode. The large irreversible capacity in the first charge/discharge cycle is due to dissolution of high-order polysulfide intermediates and the side reaction between dissolved polysulfide anions and carbonate solvent, which agrees with the CV scans. This large irreversible capacity in the first cycle was also reported in other S/C composite cathodes.[42] The irreversible capacity of Li-free S/MC in the first cycle requires an extra Li-containing anode, which will reduce the overall capacity of the full cell. The large irreversible capacity of 690 mAh/g (lithiation capacity minus delithiation capacity in the first cycles) observed in the pristine S/MC (Figure 3c) was completely compensated in the Li_2S/MC cathode. The Li_2S/MC even provides extra delithiation capacity of 100 mAh/g in the first charge/discharge cycle for the compensation of the irreversible capacity of anode couples. The amount of extra capacity of the Li_2S/MC cathode can be manipulated by adjusting the SLMP loading to match different anodes with a variety of irreversible capacities. As high-capacity anodes (such as Si and Sn) normally have large irreversible capacities, the degree of prelithiation can easily be estimated from the open-circuit potentials of prelithiated electrodes. For the as-prepared Li_2S/MC sample, the open-circuit voltage is around 1.0 V (*vs* Li/Li^+). Although the charge and discharge sequences for the Li_2S/MC are opposite those of the pristine S/MC cathodes, its potential plateaus are almost identical to those of the pristine S/MC after the first cycle (Figure 3c and d). Therefore, the Li_2S/MC cathodes synthesized *via* the *in situ* strategy can effectively preactivate the electrodes mainly because Li_2S/MC is in an expanded state. Here, it is worth noting that the discharge capacities of the Li_2S/MC electrode are higher than those of the pristine S/MC after the initial cycle and achieve more than 650 mAh/g in the second and third cycles. This indicates that *in situ* fabrication of Li_2S/MC can also improve the utilization of sulfur.

The cycling stability of the pristine and *in situ* lithiated S/MC electrodes is displayed in Figure 4, showing high Coulombic efficiency and long cycling stability for both the pristine S/MC and *in situ* lithiated Li_2S/MC electrodes. Figure 4a presents the charge and discharge voltage profiles of the S/MC electrode in the first, 10th, 200th, and 500th cycle. The S/MC maintains a capacity of 500−550 mAh/g except for the first cycle. Capacity evolution with the cycles for S/MC shown in Figure 4b demonstrates exceptional stable capacity during 800 charge/discharge cycles, which is rarely

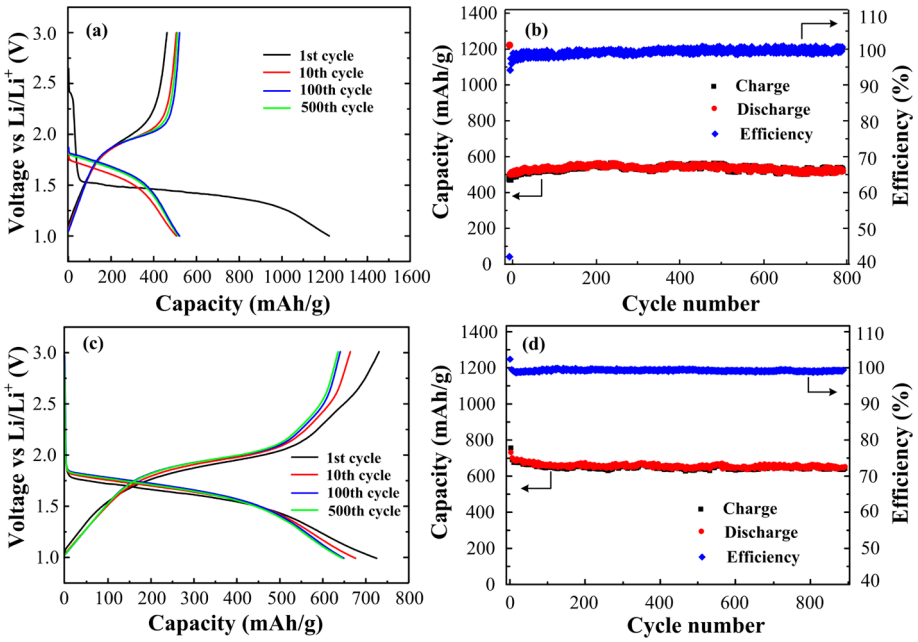

Figure 4. Cycling electrochemical properties of the S/MC and the as-prepared Li_2S/MC electrode at 0.1C: (a) discharge/charge voltage profiles of the S/MC electrode in the first, 10th, 100th, and 500th cycles, (b) cycling performance and Coulombic efficiency of the S/MC electrode, (c) discharge/charge voltage profiles of the Li_2S/MC electrode in the first, 10th, 100th, and 500th cycles, and (d) cycling performance and Coulombic efficiency of the Li_2S/MC electrode.

reported in the literature. The Coulombic efficiency is close to 100%. The long cycling stability and high Coulombic efficiency of S/MC in carbonate-based electrolytes are attributed to the elimination of high-order polysulfide intermediates, which avoids the shuttle reaction and reduces the side reaction between polysulfide anions and the carbonate solvent. The side reaction between polysulfide anions and carbonate solvent has been reported for the S_8/C cathode[45] and was confirmed using a S_8/MC composite cathode. The S_8/MC control sample was prepared by physically mixing MC and S_8 corresponding to 30% of S in MC. The long voltage plateau at 2.4−2.5 V (*vs* Li/Li^+) in the first discharge demonstrates the formation of high-order polysulfide intermediates (Figure S1). These high-order polysulfide intermediates will be dissolved into electrolyte to form polysulfide anions and react with carbonate solvent, resulting in disappearance of the 2.4−2.5 V (*vs* Li/Li^+) plateau in the second discharge and a reduced capacity from 610 mAh/g in the first discharge to 200 mAh/g in the second one.

The superior cycling stability and Coulombic efficiency of S/MC are inherited by *in situ* lithiated Li_2S/MC electrodes (Figure 4c and d), and Li_2S/MC cathodes can provide even higher capacity (650 mAh/g) than that (550 mAh/g) of S/MC (Figure 4a−d). Unlike the chemically lithiated Li_2S−C cathodes, for which a large overpotential is needed to activate the Li_2S in the first delithiation,[37,39] the delithiation potential profile of *in situ* SLMP lithiated Li_2S−C in the first cycle is similar to the behavior in the following cycles. Therefore, the Li_2S−C formed by *in situ* lithiation using SLMP is in an active state. The Li_2S/MC cathode shows minor capacity fade and around 100% Coulombic efficiency with progressive cycling for 900 times. Such electrochemical performance has not been reported for Li_2S/C cathodes to date.

The rate capabilities of the S/MC and Li_2S/MC electrodes are shown in Figure 5. The S/MC cathode provides 510 mAh/g at 0.1C (1C = 1675 mA/g) and 100 mAh/g at a high current of 10C, demonstrating a high rate performance. The prelithiated cathode of *in situ* formed Li_2S/MC shows even better rate capability than the S/MC electrode. For instance, it can provide a reversible capacity of 650 mAh/g at a current density of 0.1C and 150 mAh/g at 10C, which is around 30−50% higher than that of S/MC cathodes. Overall, the *in situ* formed Li_2S/MC electrode has a high and stable capacity together with a high rate capability.

The Li_2S/MC cathodes prepared by sulfur vapor infusion at 600 °C and *in situ* SLMP lithiation have demonstrated one of the best cycling stabilities and one of the highest Coulombic efficiencies reported in the literature. Therefore, we should expect the full cell with a Li_2S/MC cathode and Li-free anode to have a high cycling stability. A full cell using graphite as a model anode and Li_2S/MC as a cathode was assembled, and the electrochemical performance was investigated. The graphite anodes were first tested in a Li/G half-cell configuration using the same electrolyte that was utilized in the Li_2S/MC-Li half-cells. The capacity of graphite is around 270 mAh/g with a stable cycling capacity (see Figures S2 and S3). A Li_2S/MC-graphite (Li_2S-G) full cell has a capacity ratio of Li_2S/MC to G of 0.98 (Li_2S/MC is a limiting electrode).

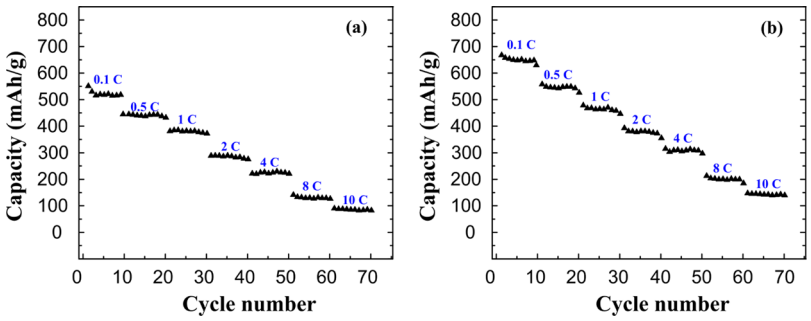

Figure 5. Rate capability curves for (a) the pristine S/MC and (b) the as-prepared Li_2S/MC electrode.

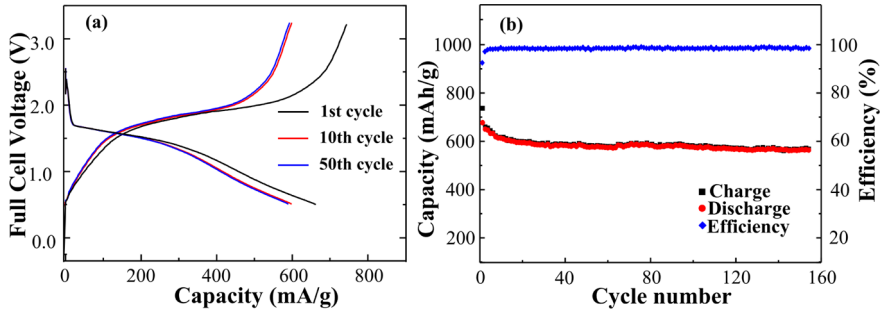

Figure 6. Electrochemical properties of the full cell with a Li_2S/MC cathode and a graphite anode: (a) discharge/charge voltage profiles in the 1st, 10th, and 50th cycle and (b) cycling performance and Coulombic efficiency curves. The specific capacity values are given with respect to the mass of Li_2S.

Figure 6a shows the voltage profiles of the first, 10th, and 50th charge and discharge cycle for a Li_2S/MC-graphite full cell at a current density of 168 mA/g. The average discharge voltage of the Li_2S-G full cell is around 1.6 V. Although a slight decay in capacity occurs in the first several cycles, the Li_2S-G full cell retains a reversible capacity of around 600 mAh/g in 150 cycles and the Coulombic efficiency is close to 100%. The irreversible capacity of the Li_2S-G full cell in the first charge/discharge cycles is less than 15% due to the extra Li in the *in situ* formed Li_2S/MC cathode (Figure 3b). The irreversible capacity of the present Li_2S/G is much lower than that (55%) of the Li_2S/Si cell.[37] The cycling test of the full cell is still under way. The electrochemical performance of the Li_2S/MC-graphite cell can be further improved by optimizing the electrode thickness and capacity ratio. The result confirms that the *in situ* fabricated Li_2S/MC electrode can not only provide the lithium source but also possess superior electrochemical performance.

CONCLUSIONS

In summary, highly stable S/MC materials were synthesized by infusing S into porous carbon at a temperature of 600 °C, and Li_2S/MC composite cathodes were fabricated by spraying SLMP onto a coated S/MC cathode electrode followed by compressing prior to cell assembly. The S/MC cathode in which S exists mainly as S_2 shows almost 100% Coulombic efficiency and provides a capacity of around 510 mAh/g without noticeable capacity decline for 800 cycles in a conventional carbonate-based electrolyte (1.0 M $LiPF_6$ + EC/DEC (1:1 v/v)). The *in situ* prelithiated Li_2S/MC cathode with an open circuit voltage of 1.0 V (*vs* Li/Li^+) shows even better electrochemical performance than that of the pristine S/MC. At a current density of 0.1C (1C = 1675 mA/g), the reversible capacities of the Li_2S/MC cathode demonstrate almost no capacity fade even on cycling up to more than 900 cycles, and the Coulombic efficiency is close to 100%. Moreover, the Li_2S/MC cathodes formed by *in situ* lithiation can pair with nonmetallic lithium anodes, such as graphite, carbon/Tin alloys, and Si nanowires through manipulating the first delithiation capacity. A Li_2S-G full cell model shows a high and stable capacity of around 600 mAh/g in 150 cycles. We believe that the results described here may substantially contribute to the progress of Li−S battery technology.

EXPERIMENTAL SECTION

Synthesis of Microporous Carbon. MC was synthesized according to a reported procedure.[41] Sucrose was dissolved in 6.0 M sulfuric acid to form a mass fraction of 5% sucrose solution, which was placed in a round-bottom flask and refluxed at 120 °C for 10 h to yield a dark brown precursor. The precursor was filtered, washed by water, and air-dried at 100 °C overnight to form a solid. Then the solid product was calcined under argon at 1000 °C for 2 h, with a heating rate of 5 °C/min.

Preparation of S/MC Composite. Identical to the procedure described in a previous publication, the S/MC composite was prepared by infiltration of sulfur into the MC.[32] In this work a mass ratio of $m_{MC}:m_S = 5:3$ was employed. The prepared MC and the sublimed sulfur (Sigma-Aldrich) were mixed by ground milling. First the mixture was sealed in an evacuated quartz tube and then heated to 600 °C at a rate of 5 °C/min and kept at this temperature for 6 h. After that, a long cooling time of 24 h was applied to ensure a complete infiltration of sulfur into the pores of MC. After cooling to room temperature, the S/MC composite was obtained. To verify the actual sulfur content in the S/MC composite, thermogravimetric analysis (TGA) was performed on a Netzsch STA 449 F1, Germany, with a heating rate of 10 °C/min, and high-purity Ar as the purge gas.

Preparation of Li_2S/MC Electrode. The S/MC composite was mixed with acetylene black and sodium carboxymethyl cellulose binder in a weight ratio of 70:15:15 mixed in distilled water. The slurry was coated on an aluminum foil to obtain a film with a thickness of approximately 40 μm, then dried in a vacuum oven at 100 °C overnight. The active material loading was around 1 mg/cm^2. Then commercialized stabilized lithium metal powder (FMC Lithium, USA), with a metallic Li content of no less than a mass fraction of 98%, was sprinkled onto the S/MC film. The SLMP loading was determined from the sulfur loading in S/MC to ensure the formation of Li_2S/MC. Due to a good stability of the SLMP, the sprinkling process was conveniently carried out in ambient conditions. The resulting film was compressed and cut into circular pieces with a diameter of 1.2 cm for assembling cells in a glovebox with an Ar atmosphere. For comparison, the film without the addition of SLMP was also compressed and cut into the same size for cell testing.

Structural Characterization. X-ray diffraction patterns were recorded on a Rigaku D/max 2400, Japan, with Cu Kα radiation in the 2-theta range from 10° to 80°. The electrode film samples after sprinkling SLMP and compressing for XRD studies were smeared on a glass slide in an argon glovebox and then covered with Scotch tape to prevent reaction with water and/or oxygen during measurement. Additionally, a fresh Al foil covered with Scotch tape was scanned in the same conditions as background (Figure S4). Scanning electron microscopy images were obtained on a Hitachi S-4700 (Japan) operating at 10 kV. The transmission electron microscope samples were examined in a JEOL (Japan) 2100F field emission TEM equipped with an energy-dispersive X-ray spectrometer.

Electrochemical Measurements. The cells were assembled in a glovebox filled with high-purity Ar. Lithium metal was used as the counter electrode and reference electrode in half-cells. Commercial graphite, Timrex KS Graphite (Timcal Group, Switzerland), was used as the anode material for full cells. The separator was mesoporous polypropylene Celgard3501 (Celgard, LLC Corp., USA). The electrolyte was 1.0 M $LiPF_6$ in a mixture of ethylene carbonate/diethyl carbonate (EC/DEC, 1:1 by volume) for both half and full cells. The charge and discharge performances of the cells were tested using an Arbin battery test station (BT2000, Arbin Instruments, USA) at room temperature. The specific capacity was calculated on the basis of the active sulfur material in half-cells. The sulfur content of the prepared S/MC composite was determined as a mass fraction of 30% by TGA; the TGA curve is shown in Figure S5. The Li_2S/MC-graphite (Li_2S-G) full cell has a capacity ratio of Li_2S/MC to G of 0.98 (Li_2S/MC is a limiting electrode). The cyclic voltammetry measurement was conducted with a Gamry Reference 3000 (Gamry Co., USA) at a scan rate of 0.1 mV/s.

Disclosure: Certain commercial equipment, instruments, or materials are identified in this work. Such identification does not imply recommendation or endorsement by the National Institute of Standards and Technology, nor does it imply that the products identified are necessarily the best available for the purpose.

Conflict of Interest: The authors declare no competing financial interest.

Supporting Information Available: Voltage profiles and discharge capacity curve of the mixed MC-S electrode, electrochemical properties of the graphite anode, XRD pattern of Al foil covered with Scotch tape, and TGA curve of the S/MC composite are available free of charge *via* the Internet at http://pubs.acs.org.

Acknowledgment. The authors gratefully acknowledge the support of the Army Research Office under Contract No. W911NF1110231 (Dr. Robert Mantz, Program Manager) and the National Science Foundation of China (No. 51272157). We acknowledge the support of the Maryland NanoCenter and its NispLab. The NispLab is supported in part by the NSF as an MRSEC Shared Experimental Facility.

REFERENCES AND NOTES

1. Herbert, D.; Ulam, J. Electric Dry Cells and Storage Batteries. U.S. Pat. 3043896, 1962.
2. Peled, E.; Gorenshtein, A.; Segal, M.; Sternberg, Y. Rechargeable Lithium-Sulfur Battery. *J. Power Sources* **1989**, *26*, 269–271.
3. Bruce, P. G.; Freunberger, S. A.; Hardwick, L. J.; Tarascon, J.-M. Li-O_2 and Li-S Batteries with High Energy Storage. *Nat. Mater.* **2012**, *11*, 19–29.
4. Diao, Y.; Xie, K.; Xiong, S.; Hong, X. Analysis of Polysulfide Dissolved in Electrolyte in Discharge-Charge Process of Li-S Battery. *J. Electrochem. Soc.* **2012**, *159*, A421–A425.
5. Ryu, H. S.; Guo, Z.; Ahn, H. J.; Cho, G. B.; Liu, H. Investigation of Discharge Reaction Mechanism of Lithium |Liquid Electrolyte| Sulfur Battery. *J. Power Sources* **2009**, *189*, 1179–1183.
6. Barchasz, C.; Molton, F.; Duboc, C.; Lepretre, J.; Patoux, S.; Alloin, F. Lithium/Sulfur Cell Discharge Mechanism: An Original Approach for Intermediate Species Identification. *Anal. Chem.* **2012**, *84*, 3973–3980.
7. Yang, Y.; Zheng, G.; Cui, Y. Nanostructured Sulfur Cathodes. *Chem. Soc. Rev.* **2013**, *42*, 3018–3032.
8. Xu, K. Nonaqueous Liquid Electrolytes for Lithium-Based Rechargeable Batteries. *Chem. Rev.* **2004**, *104*, 4303–4417.
9. Song, M.; Cairns, E. J.; Zhang, Y. Lithium/Sulfur Batteries with High Specific Energy: Old Challenges and New Opportunities. *Nanoscale* **2013**, *5*, 2186–2204.
10. Yuan, L.; Feng, J.; Ai, X.; Cao, Y.; Chen, S.; Yang, H. Improved Dischargeability and Reversibility of Sulfur Cathode in a Novel Ionic Liquid Electrolyte. *Electrochem. Commun.* **2006**, *8*, 610–614.
11. Jung, Y.; Kim, S. New Approaches to Improve Cycle Life Characteristics of Lithium−Sulfur Cells. *Electrochem. Commun.* **2007**, *9*, 249–254.
12. Zhang, S. S. Improved Cyclability of Liquid Electrolyte Lithium/Sulfur Batteries by Optimizing Electrolyte/Sulfur Ratio. *Energies* **2012**, *5*, 5190–5197.
13. Suo, L.; Hu, Y.; Li, H.; Armand, M.; Chen, L. A New Class of Solvent-in-Salt Electrolyte for High-Energy Rechargeable Metallic Lithium Batteries. *Nat. Commun.* **2013**, *4*, 1481.
14. Aurbach, D.; Pollak, E.; Elazari, R.; Salitra, G.; Kelley, C. S.; Affinito, J. On the Surface Chemical Aspects of Very High Energy Density, Rechargeable Li-Sulfur Batteries. *J. Electrochem. Soc.* **2009**, *156*, A694–A702.
15. Fanous, J.; Wegner, M.; Grimminger, J.; Andresen, A.; Buchmeiser, M. R. Structure-Related Electrochemistry of Sulfur-Poly(acrylonitrile) Composite Cathode Materials for Rechargeable Lithium Batteries. *Chem. Mater.* **2011**, *23*, 5024–5028.
16. Sun, M.; Zhang, S.; Jiang, T.; Zhang, L.; Yu, J. Nano-Wire Networks of Sulfur-Polypyrrole Composite Cathode Materials for Rechargeable Lithium Batteries. *Electrochem. Commun.* **2008**, *10*, 1819–1822.
17. Wang, J.; Yang, J.; Xie, J.; Xu, N. A Novel Conductive Polymer-Sulfur Composite Cathode Material for Rechargeble Lithium Batteries. *Adv. Mater.* **2002**, *14*, 963–965.
18. Lai, C.; Gao, X.; Zhang, B.; Yan, T.; Zhou, Z. Synthesis and Electrochemical Performance of Sulfur/Highly Porous Carbon Composites. *J. Phys. Chem. C* **2009**, *113*, 4712–4716.
19. Ji, L.; Rao, M.; Aloni, S.; Wang, L.; Cairns, E. J.; Zhang, Y. Porous Carbon Nanofiber-Sulfur Composite Electrodes for

Lithium/Sulfur Cells. *Energy Environ. Sci.* **2011**, *4*, 5053–5059.
20. Jayaprakash, N.; Shen, J.; Moganty, S. S.; Corona, A.; Archer, L. A. Porous Hollow Carbon@Sulfur Composites for High-Power Lithium-Sulfur Batteries. *Angew. Chem., Int. Ed.* **2011**, *50*, 5904–5908.
21. Weng, W.; Pol, V. G.; Amine, K. Ultrasound Assisted Design of Sulfur/Carbon Cathodes with Partially Fluorinated Ether Electrolytes for Highly Efficient Li/S Batteries. *Adv. Mater.* **2013**, *25*, 1608–1615.
22. Liang, C.; Dudney, N. J.; Howe, J. Y. Hierarchically Structured Sulfur/Carbon Nanocomposite Material for High-Energy Lithium Battery. *Chem. Mater.* **2009**, *21*, 4724–4730.
23. Ji, X.; Nazar, L. F. Advances in Li−S Batteries. *J. Mater. Chem.* **2010**, *20*, 9821–9826.
24. Manthiram, A.; Fu, Y.; Su, Y. Challenges and Prospects of Lithium-Sulfur Batteries. *Acc. Chem. Res.* **2013**, *46*, 1125–1134.
25. Bruce, P. G.; Hardwick, L. J.; Abraham, K. M. Lithium-Air and Lithium-Sulfur Batteries. *MRS Bull.* **2011**, *36*, 506–512.
26. Ji, X.; Lee, K. T.; Nazar, L. F. A Highly Ordered Nanostructured Carbon-Sulphur Cathode for Lithium-Sulphur Batteries. *Nat. Mater.* **2009**, *8*, 500–506.
27. Ding, B.; Yuan, C.; Shen, L.; Xu, G.; Nie, P.; Zhang, X. Encapsulating Sulfur into Hierarchically Ordered Porous Carbon as a High-Performance Cathode for Lithium−Sulfur Batteries. *Chem.—Eur. J.* **2013**, *19*, 1013–1019.
28. Zhang, C.; Wu, H.; Yuan, C.; Guo, Z.; Lou, X. Confining Sulfur in Double-Shelled Hollow Carbon Spheres for Lithium−Sulfur Batteries. *Angew. Chem., Int. Ed.* **2012**, *51*, 9592–9595.
29. Zhou, G.; Wang, D.; Li, F.; Hou, P.; Yin, L.; Liu, C.; Lu, G.; Gentle, I. R.; Cheng, H. A Flexible Nanostructured Sulphur-Carbon Nanotube Cathode with High Rate Performance for Li-S Batteries. *Energy Environ. Sci.* **2012**, *5*, 8901–8906.
30. Zheng, W.; Liu, Y.; Hu, X.; Zhang, C. Novel Nanosized Adsorbing Sulfur Composite Cathode Materials for the Advanced Secondary Lithium Batteries. *Electrochim. Acta* **2006**, *51*, 1330–1335.
31. Dorfler, S.; Hagen, M.; Althues, H.; Tubke, J.; Kaskel, S.; Hoffmann, M. J. High Capacity Vertical Aligned Carbon Nanotube/Sulfur Composite Cathodes for Lithium-Sulfur Batteries. *Chem. Commun.* **2012**, *48*, 4097–4099.
32. Guo, J.; Xu, Y.; Wang, C. Sulfur-Impregnated Disordered Carbon Nanotubes Cathode for Lithium-Sulfur Batteries. *Nano Lett.* **2011**, *11*, 4288–4294.
33. Cao, Y.; Li, X.; Aksay, I. A.; Lemmon, J.; Nie, Z.; Yang, Z.; Liu, J. Sandwich-Type Functionalized Graphene Sheet-Sulfur Nanocomposite for Rechargeable Lithium Batteries. *Phys. Chem. Chem. Phys.* **2011**, *13*, 7660–7665.
34. Ji, L.; Rao, M.; Zheng, H.; Zhang, L.; Li, Y.; Duan, W.; Guo, J.; Cairns, E. J.; Zhang, Y. Graphene Oxide as a Sulfur Immobilizer in High Performance Lithium/Sulfur Cells. *J. Am. Chem. Soc.* **2011**, *133*, 18522–18525.
35. Wang, H.; Yang, Y.; Liang, Y.; Robinson, J. T.; Li, Y.; Jackson, A.; Cui, Y.; Dai, H. Graphene-Wrapped Sulfur Particles as a Rechargeable Lithium-Sulfur Battery Cathode Material with High Capacity and Cycling Stability. *Nano Lett.* **2011**, *11*, 2644–2647.
36. Zhao, M.; Liu, X.; Zhang, Q.; Tian, G.; Huang, J.; Zhu, W.; Wei, F. Graphene/Single-Walled Carbon Nanotube Hybrids: One-Step Catalytic Growth and Applications for High-Rate Li-S Batteries. *ACS Nano* **2012**, *6*, 10759–10769.
37. Yang, Y.; McDowell, M. T.; Jackson, A.; Cha, J. J.; Hong, S. S.; Cui, Y. New Nanostructured Li_2S/Silicon Rechargeable Battery with High Specific Energy. *Nano Lett.* **2010**, *10*, 1486–1491.
38. Cai, K.; Song, M.; Cairns, E. J.; Zhang, Y. Nanostructured Li_2S-C Composites as Cathode Material for High-Energy Lithium/Sulfur Batteries. *Nano Lett.* **2012**, *12*, 6474–6479.
39. Guo, J.; Yang, Z.; Yu, Y.; Abruna, H. D.; Archer, L. A. Lithium-Sulfur Battery Cathode Enabled by Lithium-Nitrile Interaction. *J. Am. Chem. Soc.* **2013**, *135*, 763–767.
40. Yang, Y.; Zheng, G.; Misra, S.; Nelson, J.; Toney, M. F.; Cui, Y. High-Capacity Micrometer-Sized Li_2S Particles as Cathode Materials for Advanced Rechargeable Lithium-Ion Batteries. *J. Am. Chem. Soc.* **2012**, *134*, 15387–15394.
41. Shinkarev, V. V.; Fenelonov, V. B.; Kuvshinov, G. G. Sulfur Distribution on the Surface of Mesoporous Nanofibrous Carbon. *Carbon* **2003**, *41*, 295–302.
42. Zhang, B.; Qin, X.; Li, G.; Gao, X. Enhancement of Long Stability of Sulfur Cathode by Encapsulating Sulfur into Micropores of Carbon Spheres. *Energy Environ. Sci.* **2010**, *3*, 1531–1537.
43. Kim, J.; Lee, D.; Jung, H.; Sun, Y.; Hassoun, J.; Scrosati, B. An Advanced Lithium-Sulfur Battery. *Adv. Funct. Mater.* **2013**, *23*, 1076–1080.
44. *Sulfur, Energy, and Environment*; Meyer, B., Ed.; Elsevier: Amsterdam, 1977.
45. Gao, J.; Lowe, M. A.; Kiya, Y.; Abruna, H. D. Effects of Liquid Electrolytes on the Charge−Discharge Performance of Rechargeable Lithium/Sulfur Batteries: Electrochemical and in-Situ X-ray Absorption Spectroscopic Studies. *J. Phys. Chem. C* **2011**, *115*, 25132–25137.
46. Kasavajjula, U.; Wang, C.; Appleby, A. J. Nano- and Bulk-Silicon-Based Insertion Anodes for Lithium-Ion Secondary Cells. *J. Power Sources* **2007**, *163*, 1003–1039.
47. Guo, J.; Liu, Q.; Wang, C.; Zachariah, M. R. Interdispersed Amorphous MnO_x-Carbon Nanocomposites with Superior Electrochemical Performance as Lithium-Storage Material. *Adv. Funct. Mater.* **2012**, *22*, 803–811.